Supporting Information

Pizano et al. 10.1073/pnas.1115778108

Synthesis, Methods and Characterization

Materials. Tetrahydrofuran (THF) (99.9%, Sigma-Aldrich), dichloromethane (DCM) (99.5%, Sigma-Aldrich), acetonitrile (MeCN) (99.9%, Sigma-Aldrich), toluene (99.5%, Sigma-Aldrich), diethyl ether (Et_2O) (99.0%, Sigma-Aldrich), methanol (MeOH) (99.9%, Sigma-Aldrich), phosphorous tribromide (PBr_3) (1.0 M in DCM, Aldrich), sodium sulfate (Na_2SO_4) (anhydrous, 99%, Sigma-Aldrich), pentacarbonylchlororhenium(I) ($Re(CO)_5Cl$) (98%, Strem), 1,10-phenanthroline (phen) (99%, Aldrich), thallium(I) hexafluorophosphate(V) ($TlPF_6$) (97%, Strem), 4-pyridylcarbinol ($PyCH_2OH$) (99%, Aldrich), BL21-CodonPlus(DE3)-RIL competent cells (Stratagene), kanamycin (kan) (Sigma), Isopropyl β-D-1-thiogalactopyranoside (IPTG) (Promega), phenylmethanesulfonyl fluoride (PMSF) (Sigma), 1,4-dithiothreitol (DTT) (Promega), 5,5′-dithio-bis(2-nitrobenzoic acid) (DTNB) (Sigma), DNase I (Roche), Ni^{II}-NTA resin (Qiagen), and dimethyl formamide (DMF) (Sigma-Aldrich) were used as received. (1,10-phenanthroline)(acetonitrile)rhenium(I) hexafluorophos-phate ($[Re(phen)(CO)_3(NCMe)]PF_6$) (S1) and (1,10-phenanthroline)(4-picoline)rhenium(I) hexafluorophosphate ($[Re(phen)(CO)_3(PyCH_3)]PF_6$) (S2) were prepared as previously reported.

Physical Methods. ^1H NMR spectra were collected at the MIT Department of Chemistry Instrumentation Facility (DCIF) on a Varian Inova-500 NMR spectrometer and internally referenced to tetramethylsilane (TMS) using the proteo impurity for the deuterated solvent (d^6-acetone). UV-vis absorption spectra were obtained using a Varian Cary 5000 UV-vis-NIR spectrometer; data were collected on dilute solutions (10–50 μM) in quartz spectroscopy cells. Steady-state emission spectra were collected using a PTI QM 4 Fluorometer, which was equipped with a 150 W Xe-arc lamp for excitation and a photomultiplier tube (Hamamatsu R928) cooled to −78 °C for detection; samples were as described above for UV-vis absorption experiments. IR spectra of powder samples were recorded on a PerkinElmer Spectrum 400 FT-IR/FIR Spectrometer equipped with a Pike Technologies GladiATR attenuated total reflectance (ATR) accessory with a monolithic diamond crystal stage and a pressure clamp. Elemental analysis was performed by Midwest Microlab, LLC. ESI-MS measurements were performed by the Proteomics Core Facility at MIT. DNA sequencing was performed by the MIT Biopolymers Laboratory.

Time-Resolved Methods. Nanosecond time-resolved emission and transient absorption (TA) experiments were performed using a previously reported system (S3) with a number of significant modifications. Excitation (pump) light was provided by the third harmonic ($\lambda = 355$ nm) of a Nd:YAG laser (Quanta-Ray Lab-190-10, Spectra-Physics) with a repetition rate of 10 Hz; white light continuum (probe) was provided by a 75 W Xe-arc lamp (Photon Technologies). In the TA experiments, the probe beam was aligned directly with the sample bore while the pump beam was positioned at 15° with respect to the probe. Both beams were focused on the sample. After passing through the sample, the probe light entered a monochromator (Triax 320, Jobin Yvon Horiba) and was dispersed by a blazed grating (250 nm, 300 grooves/mm). The entrance and exit slits for the monochromator were 0.4 mm in all experiments reported herein, corresponding to a spectral resolution of 5 nm, excepting emission kinetics experiments on small molecules, which utilized 0.2-mm slits, corresponding to a 2.5-nm spectral resolution. Laser excitation energy was adjusted to 2.0 mJ per pulse for all experiments using a combination of neutral density filters and built-in pulse energy control of the Nd:YAG laser.

For single wavelength kinetics (both TA and emission), the signal was amplified by a photomultiplier tube (R928, Hamamatsu) and collected on a 1 GHz digital oscilloscope (9384CM, LeCroy); acquisition was triggered by a photodiode positioned to collect scattered pump light at the sample. Time-resolved emission experiments were performed in the same configuration; however, probe light was not used.

Transient absorption spectra were collected using a gated intensified CCD camera (ICCD) (DH520-25F-01, Andor Technology). Acquisition delays and gate times for the CCD were set by a digital delay generator (DG535, Stanford Research Systems), which is synchronized to the Q-switch output of the Nd:YAG laser. The final data were calculated from a combination of four spectra: I (pump on/probe on), I_F (pump on/probe off), I_0 (pump off/probe on), and I_B (pump off/probe off). Pump and probe beams were selectively admitted to the sample to produce these four conditions using electronically controlled fast shutters (Uniblitz T132, Vincent Associates), which were triggered by an additional digital delay generator (DG535, Stanford Research Systems), which was also synchronized to the Q-switch output of the Nd:YAG laser. The resulting TA spectrum was obtained from the calculation $\Delta OD = -\log[(I - I_F)/(I_0 - I_B)]$ to correct for sample emission and extraneous background light.

Construction, Expression, Purification, and Reconstitution of S355C–β2. Site-directed mutagenesis was performed using a Quickchange kit from Stratagene. pET15b-β2 encodes $(His)_6$-β2(C268S,C305S) (S4) and was used as the template to generate S355C mutant using primers (5′-CAATCTGCCCGACCAGATAACAACTGACTTCCACTTCC–3′ (reverse) and 5′-GGAAGTGGAAGTCAGTTGTTATCTGGTCGGGCAGATTG-3′ (forward), Invitrogen) to give S355C-β2. The mutation was confirmed by DNA sequencing at the MIT biopolymers lab. The resulting plasmid encoding S355C-β2 was transformed into competent cells (BL21-CodonPlus(DE3)-RIL), which were grown on (LB) plates (50 μg/mL kanamycin) and incubated overnight (37 °C, 12 h). A single colony was chosen and used to inoculate a small scale culture (5 mL LB, 50 μg/mL kanamycin), which was incubated with shaking (37 °C, 12 h); this subculture was subsequently used to inoculate a larger culture (100 mL LB, 50 μg/mL kanamycin, 1:100 dilution). The 100-mL culture was incubated (37 °C, 12 h) with shaking and used to inoculate cultures (2 × 2 L LB, 50 μg/mL kanamycin, 1:200 dilution), which were incubated (37 °C) with shaking. The growth of this culture was monitored by scattering at 600 nm. At an OD_{600} of ∼0.7, an aqueous solution of 1,10-phenanthroline in 0.1 M HCl (to aid in solubility) was added to a final concentration of 0.1 mM. After 15 min, overexpression was induced with IPTG (0.5 mM total concentration). After an additional 4 h, cells were harvested by centrifugation (14,000 × g, 20 min) and stored at −80 °C prior to purification (5.9 g, 1.5 g/L). Successful expression was confirmed by sodium dodecyl sulfate polyacrylamide gel electrophoresis (SDS/PAGE) of the cell lysate before and after induction (S5).

A portion of the frozen cell pellet (11.7 g) was thawed at 0 °C and resuspended in 60 mL (5 mL/g) lysis buffer (50 mM tris (hydroxymethyl)aminomethane (Tris), 500 mM NaCl, 10 mM imidazole, pH 7.6). Phenylmethanesulfonyl fluoride (PMSF) was prepared as a 20 mM stock in isopropyl alcohol (^{i}PrOH) and

added to the cell suspension to a final concentration of 200 μM. The cells were homogenized and subsequently lysed by passing through a French press (14,000 psi) twice. DNAse I (600 U, 10 U/mL lysate) was added to the suspension, which was briefly stirred (10 min, 4 °C). The mixture was centrifuged (25,000 × *g*, 25 min) to remove insoluble material. An additional aliquot of PMSF was added to the supernatant, yielding a final concentration of 400 μM.

The supernatant was slowly loaded onto a nickel affinity column (25 mL Ni^{II}-NTA resin, 1 mL/min). The flow through was reapplied to the column (7 mL/min) to ensure complete binding. The bound protein was washed with 750 mL (30 column volumes) lysis buffer (50 mM Tris, 500 mM NaCl, 10 mM imidazole, pH 7.6). The protein was then eluted with 50 mM Tris, 500 mM NaCl, 200 mM imidazole, pH 7.6 and the protein fractions combined. The imidazole was removed by Sephadex G-25 chromatography (650 mL) equilibrated with β2 buffer (50 mM Tris, 5% glycerol, pH 7.6 and concentrated to 172 μM, using $\varepsilon_{280} = 0.131\ \mu M^{-1}\ cm^{-1}$. The protein was judged to be >95% pure based on SDS/PAGE (S5).

The diferric-tyrosyl radical cofactor was reconstituted by established procedures (S6). Specifically, apo-S355C-β2 (6 mL, 172 μM in β2 Buffer) was degassed at 0 °C by alternating cycles of vacuum and argon backfill, ending with the sample under vacuum. In an glovebox under inert N_2 atmosphere, $Fe^{II}(NH_4)_2(SO_4)_2$ (160 μL, 33.6 mM, 5 equiv) was added to the degassed protein solution while stirring. The resulting solution was maintained at 4 °C (15 min). After removing the sample from the glove box, O_2 saturated β2 buffer ($[O_2] \sim 1.9$ mM, 2.7 mL, 5 equiv) was added to the sample, which was subsequently loaded on a G-25 Sephadex column (75 mL) to remove excess $Fe^{II}(NH_4)_2(SO_4)_2$. Fractions containing protein, as identified by Bradford assay, were combined and concentrated to 211 μM holo-S355C-β2. Radical content was measured using the drop line correction method (S6) and found to be 0.96/β2.

Tricarbonyl(1,10-phenanthroline)(4-hydroxymethylpyridyl)rhenium(I) Hexafluorophos-phate, [Re(phen)(CO)$_3$(PyCH$_2$OH)]PF$_6$. [Re(phen)$(CO)_3$(NCMe)]PF_6 (640 mg, 1.01 mmol, 1.0 eq) and $PyCH_2OH$ (219 mg, 2.01 mmol, 2.0 eq) were dissolved in 150 mL THF in a round bottom flask equipped with a reflux condenser, yielding a clear yellow solution. The reaction mixture was heated and maintained at reflux for 18 h. After allowing the solution to cool, the solvent was removed by rotary evaporation and the resulting oil redissolved in a minimal amount of DCM. Slow addition of 200-mL diethyl ether resulted in the formation of a bright yellow precipitate, which was isolated by vacuum filtration on a fritted funnel and left to dry overnight under vacuum (672 mg, 94%). ^{1}H NMR (500 MHz, $(CD_3)_2CO$, 20 °C): $\delta = 9.92$ (dd, 2H, phen-H), 9.10 (dd, 2H, phen-H), 8.52 (m, 2H, Py-H), 8.37 (s, 2H, phen-H), 8.35 (dd, 2H, phen-H), 7.31 (m, 2H, Py-H), 4.60-4.62 (m, 1H, OH), 4.56 (d, 2H, CH_2).

Tricarbonyl(1,10-phenanthroline)(4-bromomethylpyridyl)rhenium(I) Hexafluorophos-phate, [Re(phen)(CO)$_3$(PyCH$_2$Br)]PF$_6$ ([Re]–Br). [Re(phen)$(CO)_3$($PyCH_2OH$)]PF_6 (706 mg, 1.00 mmol, 1.0 eq) was dissolved in 100 mL DCM. The solution was cooled in an ice bath to 0 °C and a solution of PBr_3 in DCM (1.0 M, 10 mL, 10 mmol, 10 eq) was slowly added. The mixture was allowed to return to room temperature and stirred overnight. The solution was cooled on an ice bath prior to slowly adding 10 mL MeOH to quench excess PBr_3. After returning to room temperature, solvent was removed under a stream of N_2. The resulting solids were resuspended in 100 mL DCM, washed with twice with 50 mL H_2O, dried over Na_2SO_4, which was removed by filtration. The remaining solvent was removed by rotary evaporation, and the resulting solids were redissolved in 200 mL THF. To this mixture, a solution of $TlPF_6$ (3.51 g, 10 mmol, 10 eq) in 50 mL THF was added. Precipitation began immediately; the reaction was stirred overnight at room temperature. Solvent was removed from the crude reaction mixture by rotary evaporation and the resulting solids were resuspended in a minimal volume of DCM, yielding a deep yellow solution and dense white precipitate. The solid material was removed by filtration and rinsed with additional DCM. The filtrates were combined and the solvent removed. The resulting oil was redissolved in a minimal volume of DCM to which Et_2O was slowly added in excess to yield a colorless solution and yellow precipitate. The product was isolated by vacuum filtration and dried under vacuum overnight to yield [Re(phen)$(CO)_3$($PyCH_2Br$)]PF_6 ([Re]-Br) as a bright yellow powder (372 mg, 49%). ^{1}H NMR (500 MHz, $(CD_3)_2CO$, 20 °C): $\delta = 9.94$ (dd, 2H, phen-H), 9.13 (dd, 2H, phen-H), 8.66 (m, 2H, Py-H), 8.39 (s, 2H, phen-H), 8.36 (dd, 2H, phen-H), 7.45 (m, 2H, Py-H), 4.51 (s, 2H, CH_2); IR (solid, cm^{-1}): 2024, 1925, 1895 (C ≡ O stretch); Anal. calcd. for $C_{21}H_{14}N_3O_3PF_6BrRe$: C, 32.87; H, 1.84; N, 5.48; P, 4.04; Br, 10.41; found: C, 33.30; H, 2.08; N, 5.38; P, 4.23; Br, 10.27.

X-ray Crystal Structure of [Re(phen)(CO)$_3$(PyCH$_2$Br)]PF$_6$. Single crystals suitable for X-ray diffraction were obtained from vapor diffusion of Et_2O into a concentrated solution of [Re(phen)$(CO)_3$($PyCH_2Br$)]PF_6 in MeCN overnight. The crystals were mounted on a Bruker three circle goniometer platform equipped with an APEX detector. A graphite monochromator was employed for wavelength selection of the Mo Kα radiation ($\lambda = 0.71073$ Å). The data were processed and refined using the program SAINT supplied by Siemens Industrial Automation. Structures were solved by Patterson methods in SHELXS and refined by standard difference Fourier techniques in the SHELXTL program suite (6.10 v., Sheldrick G. M., and Siemens Industrial Automation, 2000). Hydrogen atoms bonded to carbon were placed in calculated positions using the standard riding model and refined isotropically.

Estimated Quantum Yield of Tyrosyl Radical Formation.

The approximate quantum yield with which •Y is generated, $\Phi_{Y\bullet}$, in [Re]-S355C-β2

$$\Phi_{Y\bullet} = \frac{\text{molecules of } \bullet\text{Y generated}}{\text{number of photons absorbed}} \qquad \textbf{[S1]}$$

under our experimental conditions may be derived from a variety of known experimental parameters. Our estimate of $\Phi_{Y\bullet}$ presumes that the entire region of the probe beam has been irradiated by the excitation laser pulse. The number of molecules of •Y generated for the observed experimental volume for a single laser flash can be calculated from Avogadro's number (N_A), the sample bore volume (V_{bore}), and the observed concentration of •Y,

$$\text{molecules of } \bullet\text{Y generated} = N_A V_{bore}[\bullet Y] \qquad \textbf{[S2]}$$

where N_A is Avogadro's number and [•Y] is determined from the intensity of the •Y signal in the transient absorption spectrum (ΔOD) and molar extinction coefficient for •Y ($\Delta\varepsilon(Y\bullet)$),

$$[Y\bullet] = \frac{\Delta OD}{\Delta\varepsilon(Y\bullet)\ell} \qquad \textbf{[S3]}$$

The number of photons absorbed can be calculated from the sample transmittance (T) and the number of photons per laser pulse (N_p).

$$\text{number of photons absorbed} = (1 - T)N_p \qquad \textbf{[S4]}$$

Substituting Eqs. **S2** and **S4** into **S1**:

$$\Phi_{Y\bullet} = \frac{N_A V_{\text{bore}}[\bullet Y]}{N_p(1-T)} \quad \textbf{[S5]}$$

The number of photons per pulse can be calculated from the laser pulse energy (E_P), the laser wavelength (λ), Planck's constant (h) and the speed of light (c).

$$N_p = \frac{E_p \lambda}{hc} \quad \textbf{[S6]}$$

Similarly, the transmittance can be calculated from the sample absorbance, which can be in turn be calculated using the Beer–Lambert law from the molar extinction coefficient for [Re]-S355C-β2 at the excitation wavelength ($(\varepsilon_{355,\text{Re-}\beta 2}$), the sample concentration ([Re-β2]), and the sample path length (ℓ).

$$T = 10^{-A} = 10^{-\{\varepsilon_{355,\text{Re-}\beta 2}[\text{Re-}\beta 2]\ell\}} \quad \textbf{[S7]}$$

Substituting Eqs. **S6** and **S7** into **S5** furnishes,

$$\Phi_{Y\bullet} = \frac{N_A V_{bore} \frac{\Delta OD}{\Delta\epsilon(Y\bullet)\ell}}{\frac{E_p\lambda}{hc}\left(1-10^{-\{\varepsilon_{355,\text{Re-}\beta 2}[Re-\beta 2]\ell\}}\right)} \quad \textbf{[S8]}$$

Evaluating with the appropriate constants (h, c, N_A) and experimental values ($V_{\text{bore}} = 70$ μL, $\Delta\text{OD} = 4 \times 10^{-3}$, $E_P = 2.0$ mJ, λ=355 nm, $\varepsilon_{355,\text{Re-}\beta 2} = 18{,}900\ \text{M}^{-1}\,\text{cm}^{-1}$, [Re -β2] = 65 μM, $\varepsilon_{\bullet Y} = 2{,}750\ \text{M}^{-1}\,\text{cm}^{-1}$ (7) and $\ell = 1$ cm) into Eq. **S7** yields $\Phi \sim 0.02 \bullet Y$.

1. Reece SY, Nocera DG (2005) Direct tyrosine oxidation using the MLCT excited states of rhenium polypyridyl complexes. *J Am Chem Soc* 127:9448–9458.
2. Cleland DM, Irwin G, Wagner P, Officer DL, Gordon KC (2009) Linker conjugation effects in rhenium(I) bifunctional hole-transport/emitter molecules. *Chem Eur J* 15:3682–3690.
3. Loh Z-H, Miller SE, Chang CJ, Carpenter SD, Nocera DG (2002) Excited-state dynamics of cofacial pacman porphyrins. *J Phys Chem A* 106:11700–11708.
4. Yee CS, Seyedsayamdost MR, Chang MCY, Nocera DG, Stubbe J (2003) Generation of the β2 subunit of ribonucleotide reductase by intein chemistry: Insertion of 3-nitro-tyrosine at residue 356 as a probe of the radical initiation process. *Biochemistry* 42:14541–14552.
5. Laemmli, UK (1970) Cleavage of structural proteins during the assembly of the head of bacteriophage T4. *Nature* 227:680–685.
6. Bollinger JM, et al. (1995) Use of rapid kinetics methods to study the assembly of the diferric-tyrosyl radical cofactor of *Escherichia coli* ribonucleotide reductase. *Methods Enzymol* 258:278–303.
7. Feitelson J, Hayon E (1973) Electron ejection and electron capture by phenolic compounds. *J Phys Chem* 77:10–15.
8. Eriksson M, et al. (1997) Binding of allosteric effectors to ribonucleotide reductase protein R1: Reduction of active-site cysteines promotes substrate binding. *Structure* 5:1077–1092.
9. Högbom M, et al. (2003) Displacement of the tyrosyl radical cofactor in ribonucleotide reductase obtained by single-crystal high-field EPR and 1.4-Å X-ray data. *Proc Natl Acad Sci USA* 100:3209–3214.

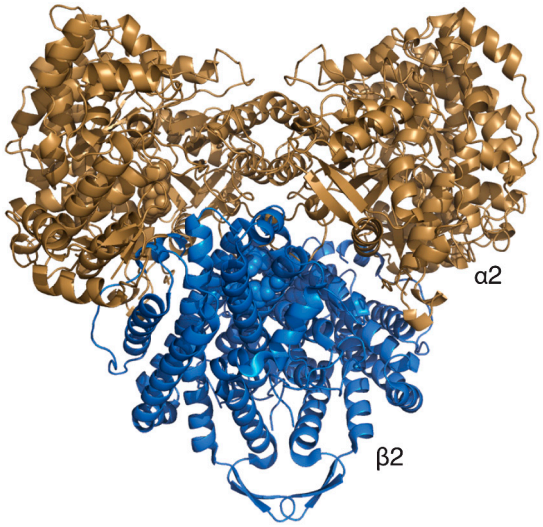

Fig. S1. Docking model for class Ia RNR. Substrate turnover requires formation of a 1:1 complex between subunits α2 (gold) and β2 (blue). A model for the active RNR complex has been proposed on the basis of reported structures for the individual subunits. Graphics were generated from Protein Data Bank entries 4R1R (α2) (S8) and 1MXR (β2) (S9).

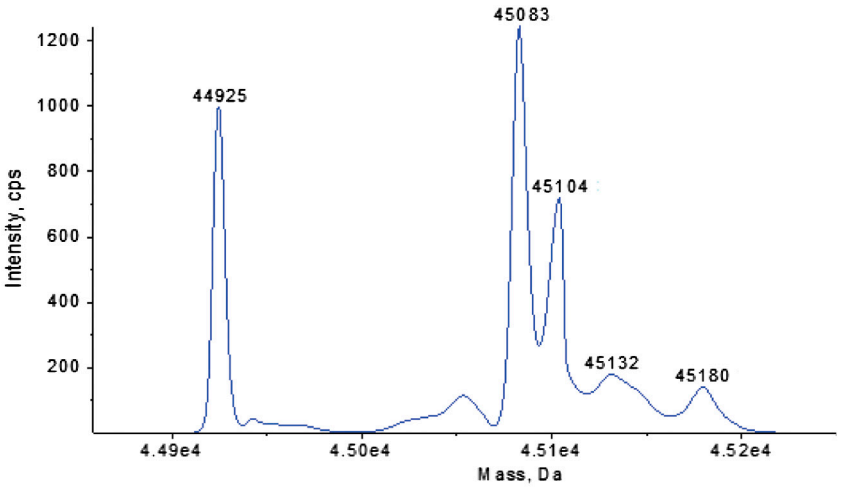

	Expected	Observed	Difference
[Re]–S355C–β2	44922.6	44925	+2.4
[Re]–fMetS355C – β2	45081.6	45083	+1.2

Fig. S2. ESI-MS spectrum for [Re]-S355C-β2. The mass spectrum of [Re]-S355C-β2 was reconstructed from ESI-MS data. The major peaks shown correspond to only expected labeled products, which include both [Re]-S355C-β2 and the *N*-formylmethionyl variant (fMet-[Re]-S355C-β2), as summarized in the following table (masses are reported in Da).

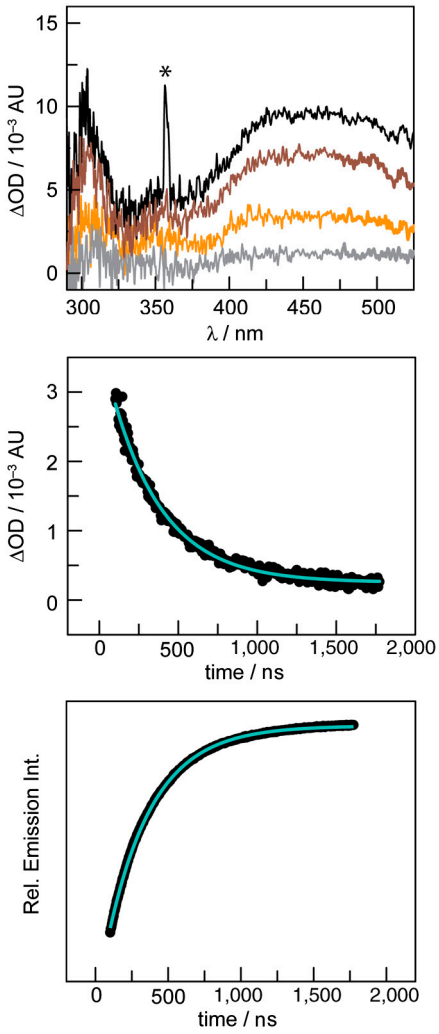

Fig. S3. Nanosecond laser flash photolysis of [Re]-S355C-β2. Time-resolved spectroscopic data are recorded after excitation ($\lambda_{ex} = 355$ nm) of [Re]-S355C-β2 (10 μM in 50 mM HEPES, 1 mM EDTA, pH 8.0). Top: Transient absorption spectra recorded 50 ns (black), 150 ns (brown), 500 ns (orange), and 1,000 ns (gray) after excitation. Spectra are collected over 50 ns, beginning at the indicated time. The observed growth features are consistent with a ^{3}[Re]* MLCT excited state. Asterisk indicates signal due to laser scatter. Middle: TA kinetics data observed at 450 nm and a monoexponential fit (green) ($\tau = 328$ ns). Bottom: Time-resolved emission data observed at 550 nm and a monoexponential fit (green) ($\tau = 311$ ns).

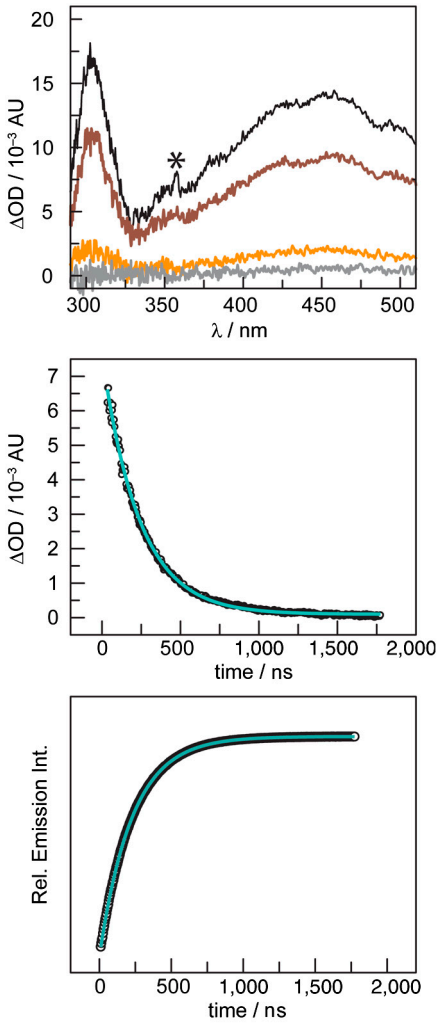

Fig. S4. Nanosecond laser flash photolysis of $[Re(phen)(CO)_3(PyCH_3)]PF_6$. Time-resolved spectroscopic data are recorded after excitation ($\lambda_{ex} = 355$ nm) of $[Re(phen)(CO)_3(PyCH_3)]PF_6$ (20 μM in MeCN). Top: Transient absorption spectra recorded 50 ns (black), 150 ns (brown), 500 ns (orange), and 1,000 ns (gray) after excitation. Spectra are collected over 50 ns, beginning at the indicated time. The observed growth features are consistent with a $^3[Re]^*$ MLCT excited state. Asterisk indicates signal due to laser scatter. Middle: TA kinetics data observed at 450 nm and a monoexponential fit (green) ($\tau = 237$ ns). Bottom: Time-resolved emission data observed at 550 nm and a monoexponential fit (green) ($\tau = 228$ ns).

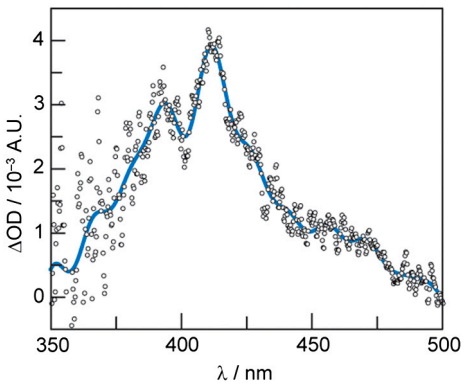

Fig. S5. As obtained transient absorption spectrum of •Y. Raw TA data (○) are shown in addition to the smoothed data (blue), as shown in the main text (Fig. 5) for reference. Experimental parameters are identical to those given in the main text. Transient absorption spectrum of [Re]-S355C-β2 collected 1 μs after 355 nm excitation (65 μM in 50 mM HEPES, 32.5 mM $Ru^{III}(NH_3)_6Cl_3$, 1 mM EDTA, pH 8.0). The spectrum shown is obtained from 2,500 four-spectrum sequences taken on two samples (1,250 four-spectrum sequences each), averaged, and smoothed using a low-pass filter on the basis of a fast Fourier transform (FFT).

Table S1. Selected crystal data and structure refinement parameters for [Re]-Br

	$[Re(phen)(CO)_3(PyCH_2Br)]PF_6 \bullet 0.5MeCN \bullet 0.5Et_2O$
Empirical formula	$C_{24}H_{20.5}BrF_6N_{3.5}O_{3.5}PRe$
Formula weight (g/mol)	825.02
Temperature	100(2) K
Crystal system	Triclinic
Space group	*P*1
Color	yellow
a (Å)	10.8930(10)
b (Å)	13.1684(12)
c (Å)	19.5663(17)
α (°)	88.257(2)
β (°)	87.481(2)
γ (°)	78.978(2)
V (Å^3)	2,751.5(4)
Z	4
No. of reflections	61,891
No. of unique reflections	15,328
R_{int}	0.0424
*R*1* (all data)	0.0553
*wR*2 [†] (all data)	0.1079
*R*1 [($I > 2\sigma$)]	0.0393
*wR*2 [($I > 2\sigma$)]	0.0986
GOF [‡]	1.029

*$R1 = \sum ||F_o| - |F_c|| / \sum |F_o|$.
†$wR2 = (\sum(w(F_o^2 - F_c^2)^2) / \sum(w(F_o^2)^2))^{1/2}$.
‡$\text{GOF} = (\sum(w(F_o^2 - F_c^2)^2)/(n-p))^{1/2}$ where n is the number of data and p is the number of parameters refined.

Table S2. Selected metric parameters for [Re]-Br

Re(1)-N(1)	2.218(5)	C(1)-O(1)	1.137(7)
Re(1)-N(2)	2.193(4)	C(2)-O(2)	1.151(7)
Re(1)-N(3)	2.179(4)	C(3)-O(3)	1.158(7)
Re(1)-C(1)	1.931(6)	N(1)-Re-N(2)	83.12(15)
Re(1)-C(2)	1.931(5)	N(1)-Re-N(3)	88.99(15)
Re(1)-C(3)	1.926(5)	N(2)-Re-N(3)	75.41(15)

Distances are reported in Å; angles are reported in degrees.